The 11th Canadian Conference on Earthquake Engineering
Canadian Association for Earthquake Engineering

Compression Failure of RC Beams Deteriorated by Corrosion

Ryo MURAI
Master Program, University of Tsukuba, Japan
s1420936@u.tsukuba.ac.jp

Michiaki OYADO, Dr.Eng.
Senior Researcher, Railway Technical Research Institute, Japan
oyado@rtri.or.jp

Akira YASOJIMA, Ph.D.
Assistant Professor, University of Tsukuba, Japan
yasojima@kz.tsukuba.ac.jp

Toshiyuki KANAKUBO, Ph.D.
Associate Professor, University of Tsukuba, Japan
kanakubo@kz.tsukuba.ac.jp

ABSTRACT: It is important to clarify the degradation of structural performance of existing reinforced concrete (RC) structures to manage the sustainable infrastructures. Typical factor of deterioration is corrosion of reinforcing bar. Many studies have been conducted about the effects of reinforcing bar corrosion on the structural performance of RC members. Because corrosion of reinforcing bars has large influence on the safety, it is necessary to accurately assess the effects of degradation. The bending capacity of RC beam is influenced only by the characteristics of tension bars, deformation capacity is affected by compressive performance of concrete. The objective of this study is to investigate the influence of compression failure of concrete to the performance of RC member. RC beam specimens, in which the corrosion of compression bars and cracks in compression region are simulated, are subjected to bending test. As the test results, it is recognized that the damages in compression region cause the remarkable decrement of deformation capacity of RC beams. Load–deflection curves of the specimens are simulated by the section analysis. In the analysis, buckling of compression bars and deterioration of compression performance of concrete are considered. The analysis results show a good agreement with the experimental ones.

1. Introduction

It’s important to clarify the degradation of structural performance of existing reinforced concrete (RC) structures to manage the sustainable infrastructures. Typical factor of deterioration is corrosion of reinforcing bar. Many studies have been conducted about the effects of reinforcing bar corrosion on the structural performance of RC members. Because corrosion of reinforcing bars has large influence on the safety, it is necessary to accurately assess the effects of degradation. Corrosion of reinforcing bars causes the degradation of bending and shear capacity of RC members. The reduction of cross-sectional area of corroded bars exhibits the degradation of yield and tensile strength of the bars and causes remarkable decrement of deformation capacity. In addition, cracks along the reinforcing bars due to corrosion lead to the transition of failure mode of RC member such as bond splitting failure. These phenomena have been studied in many previous researches. Cracks along the reinforcing bars have a possibility to lead the degradation of concrete performance. While the bending capacity of RC beam is influenced only by the characteristics of tension bars, deformation capacity is affected by compressive performance of concrete (Oyado et al., 2006). The objective of this study is to investigate the influence of compression failure of concrete to the performance of RC member.

The objective of this study is to investigate the influence of compression failure of concrete to the performance of RC member. RC beam specimens, in which the corrosion of compression bars and cracks in compression region are simulated, are subjected to bending test. The experimental load-deflection curves are simulated by section analysis using stress-strain model of cracked concrete and the reinforcing bars in buckling. To obtain the stress-strain curves of buckling bars, the buckling test is also conducted.

2. Experiment Program

The beam specimen is shown in Fig. 1. Mechanical properties of used materials are shown in Table 1 and Table 2. Specimens with cross section of 150mm × 235mm are subjected to four point bending test. The pure bending span is 400mm. The specimens are reinforced with high tensile strength reinforcing bars, and low strength concrete is used in order to ensure that the failure of concrete in compression side occurs first. Specimens list is shown in Table 3. Variation factors are the simulation method of concrete crack and sectional area reduction in compression bars. The concrete crack is simulated by inserting slits around the compression bars in pure bending span. Fig. 2 shows the variation of slits. The acrylic sheets are set in the beam side in full region of pure bending span in specimens B-Sc and B-Sc(R). The 50 mm long sheets are set in same region with the intervals of 100 mm in specimen B-Si. In specimen B-US, the 50 mm long sheets are set both in the beam side and upper.

The sectional-area reduction due to corrosion is simulated by scraping the reinforcing bar. The bars are scraped using a disc sander as shown in Fig. 3. Scraping is carried out by controlling a scraped depth in the minimum diameter direction between lugs of reinforcing bar. An ellipse having a nominal cross-sectional area is assumed to determine cross-sectional area ratio, which is set to be 30%. The scraped positions are set in the pure bending span as shown in Fig. 1. The last letter (R) in specimen ID shows that the specimens have scraped compression bars.

Monotonic loading is carried out using a universal testing machine of 2,000kN capacity, Measurement items are applied force, deflections at loading points, and strains of reinforcing bars as indicated in Fig. 1.

Table 1 – Mechanical property of concrete

Compressive strength (MPa)	Strain at compressive strength (%)	Elastic modulus (GPa)	Splitting strength (MPa)
12.8	0.21	20.6	1.46

Table 2 – Mechanical property of reinforcing bars

Type	Yield strength (MPa)	Yield strain (%)	Elastic modulus (GPa)	Remarks
D10	385	0.21	185	Compression bars
D16	597	0.29	201	Tension bars

Table 3 – Specimens list

ID	Section and rebars	Damage simulation of concrete	Damage simulation of bars
B-N	Cross-section 235 mm × 150 mm Tension bars 3-D16 Compression bars 2-D10	No damage	No damage
B-N(R)		No damage	Scraped 30%
B-Sc		Side cracks (full)	No damage
B-Sc(R)		Side cracks (full)	Scraped 30%
B-Si		Side cracks (half)	No damage
B-US		Upper and side cracks (both half)	No damage

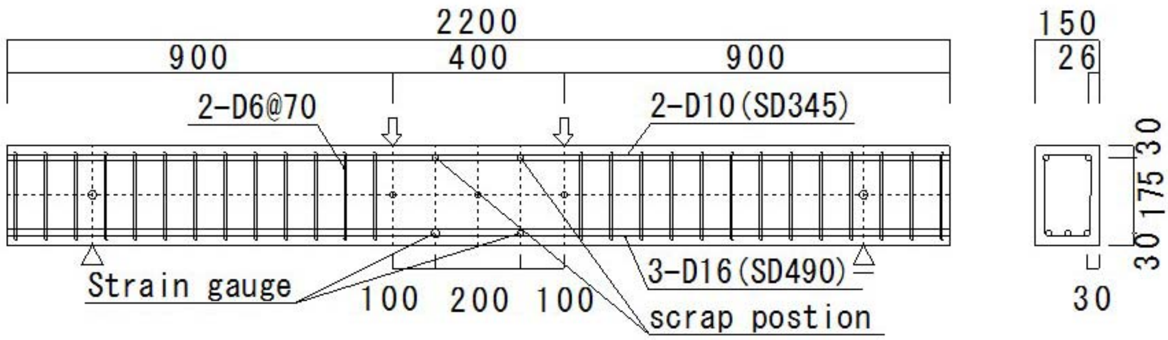

Fig. 1 – Dimensions of specimen (unit in mm)

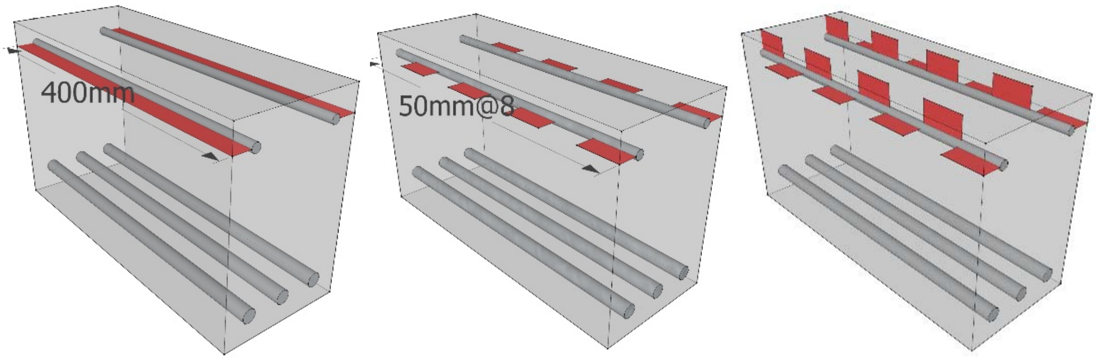

Fig. 2 – Crack of cover concrete by slits (left : B-Sc center : B-Si right : B-US)

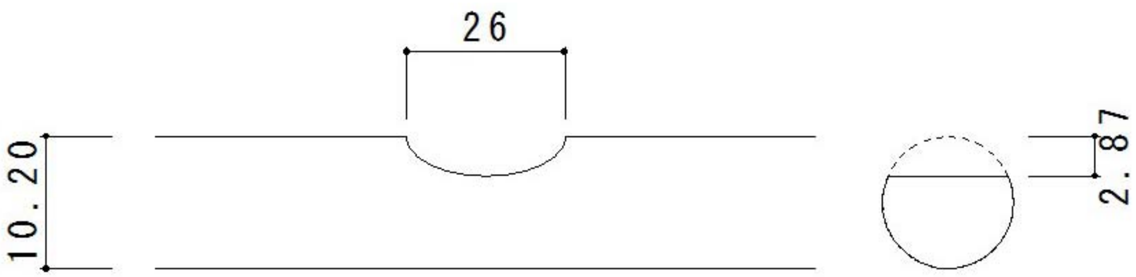

Fig. 3 – Scraping of reinforcing bar (unit in mm)

3. Test Results

Final crack patterns of specimens are shown in Fig. 4. Compression failure occurred in the shear span in specimens B-N and B-Si, while it is observed in pure bending span in other specimens. Compression reinforcing bars showed buckling with the deformation toward the outside of cross-section of beams. Load-deflection curves of specimens are shown in Fig. 5. The remarkable drop of applied load and brittle behavior can be observed in the specimens with compression failure in pure bending span. The influence of types of damage of concrete on the load-deflection curve is recognized.

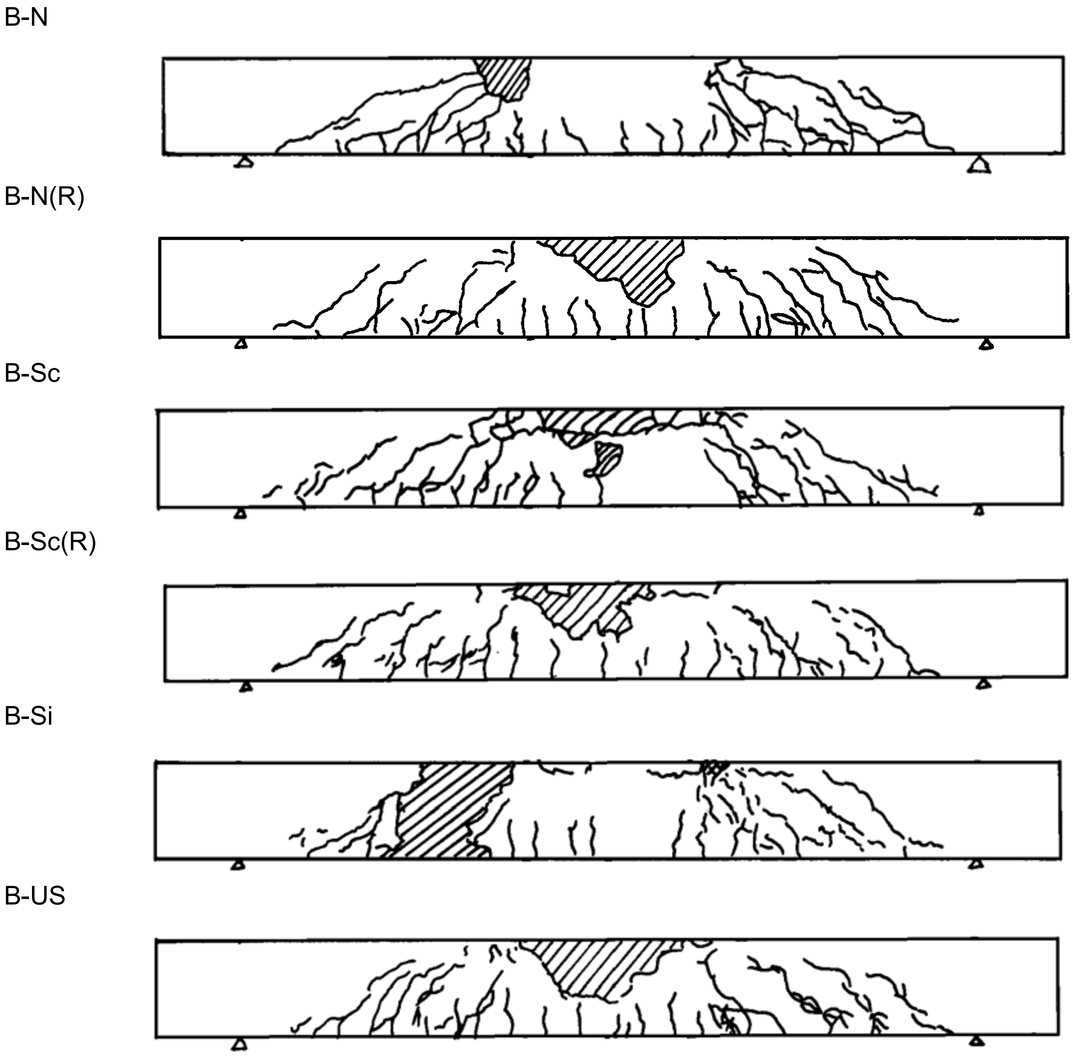

Fig. 4 – Final crack pattern

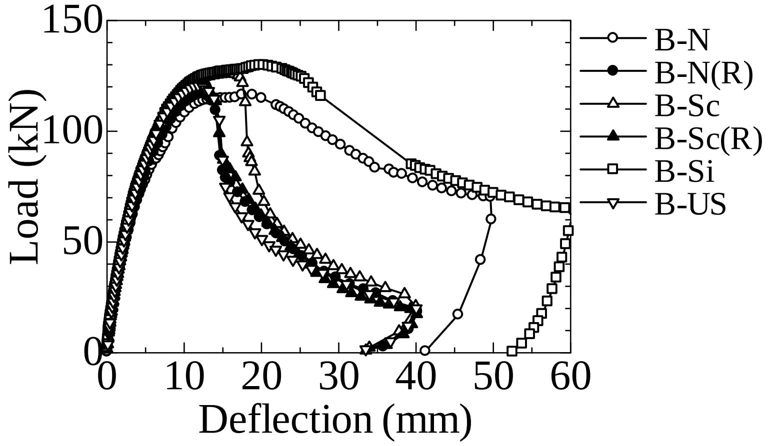

Fig. 5 – Load-deflection curve

4. Modeling of Stress-Strain Curves and Section Analysis

4.1. Buckling Test and Modeling of Reinforcing Bar

Monotonic compression loading is carried out using a universal testing machine of 500kN capacity to obtain stress-strain curve of reinforcing bars in buckling. The jigs for fixing specimen are attached to the heads of the testing machine, so the boundary condition is to be fixed-end by inserting the ends of 8*d* of the reinforcing bar in the jigs. The inserted ends of reinforcing bar are polished to produce no gap between the holes of the jigs and the reinforcing bar. The test length is set to 400 mm which is same length with pure bending span of the beam specimen. Measurement items are compressive force and an axial deformation using LVDTs in three positions between the jigs.

Stress-strain curves measured in loading test are shown in Fig. 6. Stress is determined by dividing compressive force by the nominal cross-sectional area. Strain is calculated by dividing axial deformation in test region by test length. The deformation in test region is obtained by subtracting the deformations of the bar in the hole (assumed as elastic) from the measured deformation by LVDT. Slenderness ratio of the specimen is approximately 200, so the elastic bucking occurred. The measured post-peak curves show similar with previous study (Suminokura et al., 2015) in which the post-peak curves are modeled by Equation (1). In this study, the experimental coefficient β is modified as 0.568.

$$\sigma_s = \sigma_{s\max} \times \left(\frac{\varepsilon_{s\max}}{\varepsilon_s}\right)^{\beta \times \left(1-\frac{\gamma}{100}\right)^{0.5}} \quad (1)$$

Where,

σ_{smax} : maximum stress of reinforcing bar

ε_{smax} : strain at the maximum stress

β : experimental coefficient

γ : cross-section reduction rate

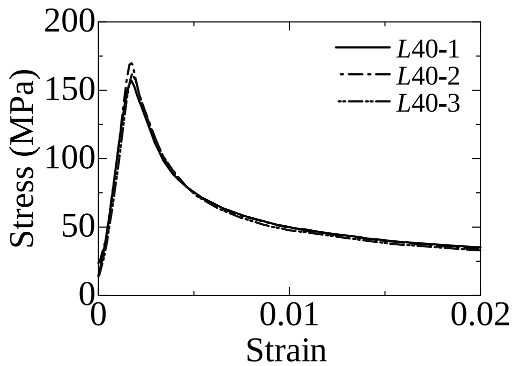

Fig. 6 – Stress-strain curve in buckling test

4.2. Modeling of Concrete

The stress-strain model of concrete is described in Equation (2) based on Popovics model, considering the influence of slits simulating cracks due to corrosion. Coefficient α is newly introduced to express the difference of shape of curves after maximum stress. Coefficient α is given as the ratio of summation length of slits to target length (pure bending span). Fig 7 shows the stress-strain curves comparing the influence of the coefficient. As the value of α increases, post-peak curves become more brittle. For specimens B-Sc and B-US, α is 1.0 and for specimen Si, α is 0.5.

$$\sigma_c = \sigma_{c\max} \times \frac{\varepsilon_c}{\varepsilon_{c\max}} \times \frac{n}{n-1+\left(\frac{\varepsilon_c}{\varepsilon_{c\max}}\right)^n} \quad (2)$$

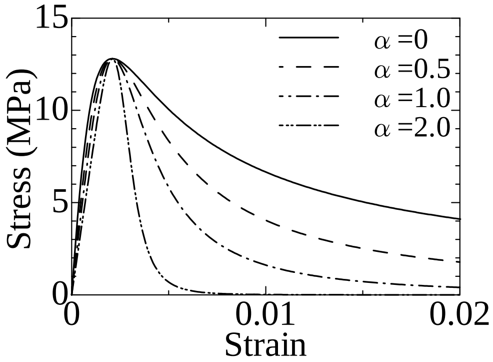

Fig. 7 – Stress-strain model of concrete

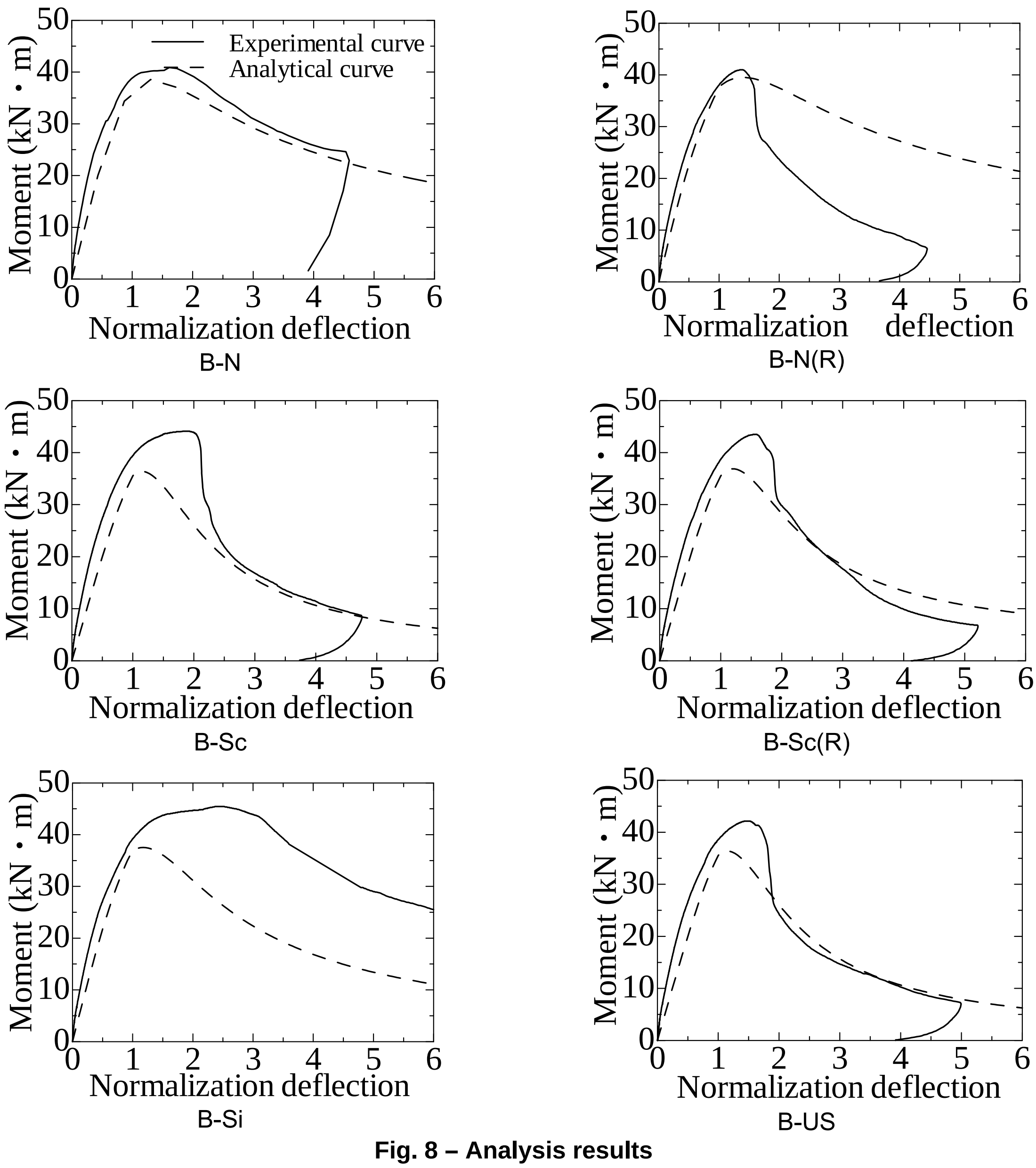

Fig. 8 – Analysis results

$$n = \frac{0.0582}{e^{-\alpha}} \times \sigma_{c\max} + 1$$

$$\alpha = \frac{L_{cr}}{L}$$

Where,

σ_{cmax} : maximum stress of concrete

ε_{cmax} : strain at the maximum stress

α : coefficient for influence of cracks

L : target length (pure bending span)

L_{cr} : Sum of crack length in the target

4.3. Comparison of Test Result with Analysis

Section analysis using proposed stress-strain models is carried out based on the assumption that the plain section remains plain. To compare between the curvature of analysis results and the deflection of experimental results, each value is normalized by ones when the strain of tension bar reaches 2000μ. The moment-normalized deflection curves are shown in Fig. 8. Analytical curves excluded specimens B-N(R) and B-Si can follow the experimental ones in the post-peak curves. Analytical curves of specimens B-N (R) and B-Si do not show good agreements with the experimental curves because of the failure at shear span.

5. Conclusion

(1) The remarkable drop of applied load and brittle behavior can be observed in the specimens with compression failure in pure bending span. The influence of types of damage of concrete on the load-deflection curve is recognized.

(2) The stress-strain curves both for cracked concrete and buckling reinforcing bars are modeled. The analytical curves calculated by section analysis can follow the experimental ones in the post-peak curves.

6. Acknowledgements

This study was supported by the JSPS KAKENHI Grant Number 24560593.

7. References

SUMINOKURA, Shun, KANAKUBO, Toshiyuki, OYADO, Michiaki, YASOJIMA, Akira, “Study on Simulated Corrosion Reinforcing Bars Subjected to Buckling Behavior”, *Proceedings of the Japan Concrete Institute* Vol.37, 2015.(in Japanese)

OYADO, Michiaki, KANAKUBO, Toshiyuki, YAMAMOTO, Nobuyuki, SATO, Tsutomu, ”Influence of Corrosion of Reinforcing Bars on Bending Performance of Reinforced Concrete Members”, *JSCE Journal of Materials, Concrete Structures and Pavements*, Division E, Vol.62, No.3, August 2006, pp. 542-554. (in Japanese)